Use of parabolic reflector to amplify in-air signals generated during impact-echo testing

Xiaowei Dai, Jinying Zhu,[a] and Yi-Te Tsai
Department of Civil, Architectural and Environmental Engineering, The University of Texas at Austin, Austin, Texas 78712
xdai@utexas.edu, jyzhu@mail.utexas.edu, ytt@utexas.edu

Michael R. Haberman
Applied Research Laboratories, The University of Texas at Austin, P.O. Box 8029, Austin, Texas 78713-8029
haberman@arlut.utexas.edu

Abstract: The impact-echo method is a commonly used nondestructive testing technique for elastic plates in civil engineering. The impact-echo mode corresponds to the frequency at zero group velocity of S_1 Lamb mode. Recent development of the air-coupled impact-echo (ACIE) method introduces the possibility for rapid scanning of large structures and increases the practicality of *in situ* measurements. However, sensors used in ACIE are susceptible to ambient noise, which complicates *in situ* ACIE measurements. This letter presents the results of ACIE measurements taken using a parabolic reflector together with standard measurement microphones to increase the signal to noise ratio for ACIE measurements. The signal gain and effects of sensor location with respect to impact location are discussed.

PACS numbers: 43.40.Dx, 43.20.Mv, 43.35.Yb [JGM]
Date Received: June 20, 2011 **Date Accepted:** July 18, 2011

1. Introduction

The impact-echo (IE) method has been a commonly used nondestructive testing (NDT) method for concrete structures since it was developed in 1980s (Sansalone and Carino, 1986). The technique measures the transient response of an elastic plate subjected to an impact, and finds the peak frequency of the resulting signal amplitude spectrum. The plate thickness and location of a defect can be estimated from the peak frequency when the material properties are known. Although the IE mode was typically interpreted as a thickness resonance associated with multiple reflections of P waves between two surfaces of a plate, Gibson and Popovics (2005) employed Lamb wave theory to show that the IE frequency coincides with an S_1 mode that has zero-group-velocity (ZGV). This fundamental explanation of IE behavior successfully explained the ad hoc shape factor β commonly employed for different materials and geometries. Expanding on this work, Prada *et al.* (2008) have shown that the β-factor is related to the Poison's ratio of the plate material and that many Lamb modes will display this useful ZGV behavior under precise conditions. Of interest for NDT community is the fact that when this ZGV mode is generated, wave energy is trapped locally near the source point leading to strong out-of-plane motion that efficiently radiates acoustic waves into air. Holland and Chimenti (2003) have successively generated and measured the S_1ZGV Lamb wave using the air coupled sensors. Other kinds of noncontact sensors such as heterodyne interferometer (Clorennec *et al.*, 2007) have also be applied to measure ZGV modes.

The IE method has found widespread use for scanning large scale civil engineering structures. However, traditional contact testing methods are slow due to the

[a]Author to whom correspondence should be addressed.

requirement of physical coupling between the sensors and the test surface. Despite the huge acoustic impedance mismatch between the concrete and air, recent research has shown the effectiveness of air-coupled sensing for concrete NDT. Zhu and Popovics (2002, 2005, 2007) employed microphones to detect propagating leaky surface waves and IE resonance generated by a point impact applied to a concrete plate. However, due to the omnidirectionality of many microphones and the common IE frequencies of concrete structures (below 30 kHz), the ambient noise level often overcomes the IE signal radiated into the air. This letter investigates the use of acoustic focusing reflectors to improve the IE signal quality for ACIE testing. The experimental studies presented here show signal enhancement attributed to the combination of focusing effect of the reflector and multiple reflections of waves between the reflector and the test surface.

2. The pressure field in air generated by ZGV modes

Lamb waves are guided acoustic waves in solid plates. Figure 1(a) shows the dispersion curves of the first three modes of Lamb waves in a concrete plate. The phase velocity is known to be $V_{ph} = \omega/k = f\lambda$ and the group velocity, $V_g = d\omega/dk = df/d(1/\lambda)$, is determined by the slope of the dispersion curves in Fig. 1(a) at a given point. Prada *et al.* (2008) found that the existence of ZGV Lamb modes depends on the Poisson's ratio, υ, of the plate material. Their work showed that the S_1ZGV Lamb mode exists in most materials with $\upsilon \leq 0.45$, while the A_2ZGV mode exists for $\upsilon \leq 0.319$. For reference, two ZGV points corresponding to the zero-slope condition of the S_1 and A_2 Lamb mode curves are marked with circles in Fig. 1(a).

At a ZGV point, the Lamb wave has nonzero phase velocity, but the group velocity is zero. The energy associated with wave motion at this frequency is therefore trapped in an area localized near the excitation. The resulting out-of-plane motion of this mode continuously radiates acoustic waves into the air until the energy is lost due to acoustic radiation or internal dissipation (Holland and Chimenti, 2004). The numerical simulation shown in Fig. 1(b) supports this assertion. In the simulation, a point impact loading is applied on the surface of a concrete slab. Acoustic waves are radiated into the air at an angle that depends upon the phase velocity of the mode at the air–plate interface.

In the example shown in Fig. 1, the concrete specimen has a thickness of 0.19 m, a measured *P*-wave velocity of 4086 m/s, and a Poisson's ratio 0.22. The associated S_1ZGV frequency is 10.2 kHz at $h/\lambda = 0.29$, which gives a phase velocity of $V_{ph} = 6704$ m/s. Using the Snell's law one finds the radiation angle of the S_1ZGV resonance to be $\theta = \text{asin}(V_{\text{air}}/V_{ph}) = 2.9°$. For *in situ* testing, such a small angle has little effect on the measured response so the S_1ZGV wave in air could reasonably be considered a plane wave propagating normal to the test surface. Similarly, the A_2ZGV resonance at 18.9 kHz also radiates plane wave into air almost normal to the plate surface (1.9°). This property of ZGV modes provides the basis to amplify IE test signals by

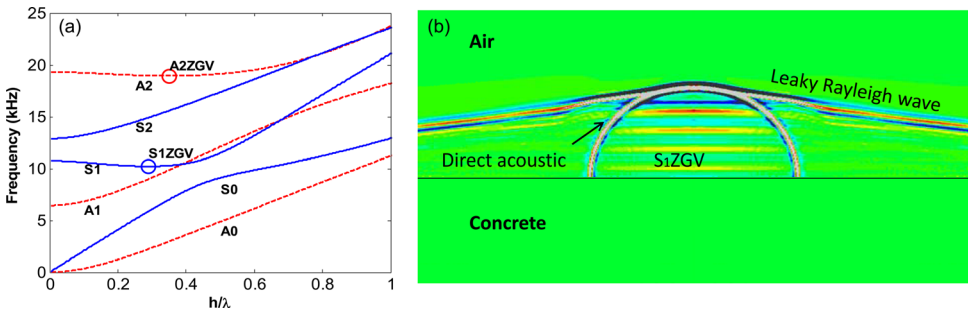

Fig. 1. (Color online) (a) Lamb wave dispersion curves for the first three symmetric and antisymmetric modes. (b) The numerical simulation of pressure field generated by an impact force acting on a concrete plate.

using a parabolic reflector whose axis is normal to the plate surface to focus the incoming plane wave. It is important to note that the S_1ZGV mode shape given by Gibson and Popovics (2005) could be approximated by a zero order Bessel function of the first kind. Given this information, the dimensions of the reflector should be selected based on expected S_1ZGV frequencies relevant to the application such that only acoustic radiation resulting from motion within the first nodal point is captured.

3. The parabolic focusing reflector

A parabolic focusing reflector has been chosen to transform the acoustic signal radiated by the ZGV mode into a spherical wave that converges near the geometric focus of the reflector. In so doing, the reflector gathers the acoustic energy that intercepts its cross-section and redirects it to the focal point, leading to significantly increased signal amplitude. The IE test also generates other types of waves in air, namely a spherically spreading in-air wave (direct wave), and a leaky surface wave, which is a quasiplane wave propagating at the Rayleigh angle. One benefit of the parabolic reflector is that it only effectively focuses plane waves parallel to its axis of revolution. In this sense, the reflector acts as a filter that selects the ZGV mode and amplifies its level.

Another useful attribute of a parabolic reflector is that its presence will lead to multiple reflections of the ZGV waves between the reflector and the testing surface. Path 1 in Fig. 2(a) is the reflection between the top portion of the reflector and the plate surface, which act approximately as two parallel walls. Path 2 exists when a reflector has its focal point above the edge level or when the impact has offset from the reflector axis. The existence of these multipath phenomena when the reflector is present mean that the microphone receives the ZGV signal multiple times which results in a cumulative increase in acoustic energy at the ZGV frequency, further increasing SNR for the air-coupled measurement.

4. Experimental procedures and results

4.1 Test setup

All tests were performed on a concrete specimen of 0.19 m thick, with lateral dimensions of 1.5 m $\times$ 1.5 m. The measured *P*-wave velocity in concrete is 4086 m/s. In this study, a parabolic reflector is included above a measurement microphone such that the sensor diaphragm is located at the geometric focus. The dimensions of the aluminum parabolic reflector are shown in Fig. 2(a). The reflector was supported on wood blocks to maintain a specified height (H). A PCB426B03 microphone attached to a PCB 480B21 signal conditioner was used to detect in-air signals. The microphone has a 6.3 mm diameter and a flat sensitivity response of 4 mV/Pa over a broad frequency range (4 – 80 kHz at $\pm$ 2dB). The broad range frequency response and high sensitivity ensure

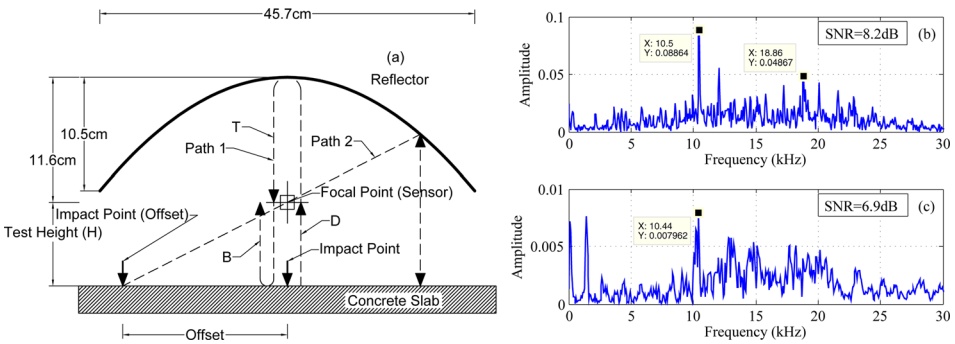

Fig. 2. (Color online) (a) Parabolic reflector. (b) The IE spectra measured by a microphone with the reflector and (c) without the reflector. Both signals were taken at an offset of 40 cm from the impact. The microphone heights from the slab surface were 6.6 and 0.5 cm in (b) and (c). The band averaged SNR for the S_1ZGV mode is shown in the figure.

detection of all ZGV modes of interest in concrete structures, which is the focus of this study. The output from the signal conditioner is digitized and captured by a digital oscilloscope (NI USB-5133) and analyzed in the time and frequency domains on a PC using a Labview program. The sampling frequency of all tests was 1 MHz and 10 000 data points were recorded for each test, equivalent to a 10 ms record length.

A steel ball mounted on a rod was used as an impactor to manually generate elastic waves in the concrete specimen. When test height effect was investigated, the impact was located directly below the sensor to minimize the effects of leaky surface wave interference on the results. In the offset effect study, impacts were located at different distances from the acoustic axis of the sensor.

4.2 Amplification effect of the reflector

To evaluate the performance of the reflector, a test was performed to compare signals measured by a microphone with the reflector (Mic 1), and one without (Mic 2). The liftoff distances for both sensors were 6.6 cm (Mic 1) and 0.5 cm (Mic 2) from the slab surface. Mic 2 was enclosed in a cylinder of foam insulation to block the direct wave and ambient noise. Both sensors were placed at the same distance from the impacting point, and simultaneously measured signals generated by one impact. Representative signal spectra are shown in Figs. 2(b) and 2(c). Both measurements show a sharp peak around 10.5 kHz, which matches the predicted S_1ZGV frequency (10.2 kHz) in Sec. 2. However, the ratio of the peak amplitude between two signals measured by Mic 1 and Mic 2 is around 11, corresponding to approximately 20 dB signal gain with the reflector. In addition, the measurement with Mic 2 also shows another peak around 19 kHz, which agrees with the A_2ZGV frequency and reinforces the assertion that the reflector effectively focuses the quasiplane ZGV waves. Further, these results show that the reflector has improved the air-coupled sensing capability of the system. One observes a band averaged SNR of 8.2 dB in Fig. 2(b), which corresponds to an improvement of 1.4 dB by using the reflector. In addition, the S_1ZGV mode peak is more prominent in Fig. 2(b) relative to other peaks.

4.3 Test height effect

A previous ACIE study (Zhu and Popovics, 2007) required small separation between the microphone and the slab to mitigate attenuation of impact-echo signal level due to absorption and spreading. For *in situ* testing, however, a higher liftoff distance is desirable to prevent microphone damage. In addition, the microphones may not be accurately maintained at a fixed height during testing. For these reasons, the effect of test heights is reported in this letter.

A series of tests with different sensor height, H, were conducted with the same parabolic reflector and microphone. An accelerometer near the impact point was used to provide the trigger signal. The results are shown in Fig. 3 where the y axis shows the sensor height from the concrete surface. The time domain signals in Fig. 3(a) show the expected arrival times of the acoustic wave and its multiple reflections from the plate (B) and the reflector (T) are plotted with the dashed lines. The reflection from the reflector (T) is much stronger than the plate reflection (B) due to the focusing effect. The frequency spectra in Fig. 3(b) show that this reflector system is able to identify the S_1ZGV frequency from a significant offset height. To illustrate the contribution of multiple reflections to the S_1ZGV signal, Fig. 3(c) shows a complex Morlet wavelet spectrogram of the signal at 40 cm height. This plot clearly shows that the signal at 10 kHz contains nonnegligible levels after 5 ms due to the second reflection from the reflector, which provides enhancement of the S_1ZGV amplitude in the frequency domain.

4.4 Offset distance effect

Practical implementation of the ACIE test requires that the impact point be located at some offset distance from the sensor axis to permit excitation in the presence of the

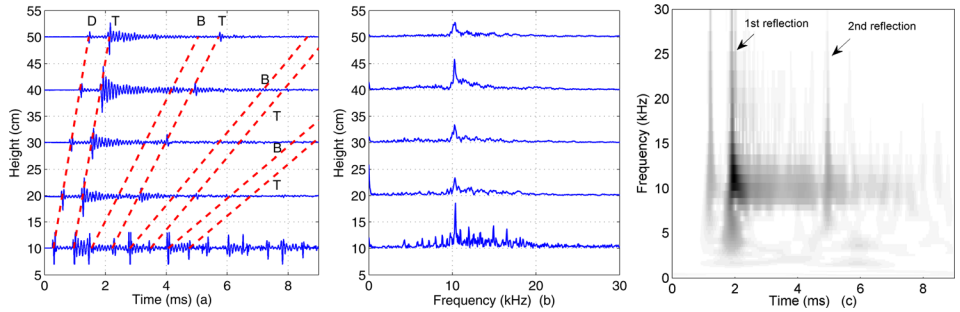

Fig. 3. (Color online) (a) Time domain signals and (b) frequency spectra from different test heights. The dashed lines and labels represent arrival times of the direct acoustic wave (*D*), its reflection from the top reflector (*T*), and from the bottom slab surface (*B*). (c) Spectrogram of a complex Morlet wavelet analysis of the 40 cm offset height indicates significant S_1ZGV signal level out to nearly 8 ms.

reflector or insulation. However, Gibson and Popovics (2005) indicated that the signal amplitude generated by the S_1ZGV mode will decreases with distance from the excitation point. The source-to-receiver spacing, which is the impact offset distance shown in Fig. 2(a), is therefore expected to affect the S_1ZGV signal quality. To investigate the offset effect when using a parabolic reflector, signals gathered from different offset distances were collected with the sensor height maintained at 27.5 cm. An accelerometer was placed directly below the microphone to provide a trigger signal and normalization. Figure 4(a) shows measured time domain signals, the expected arrival times of the leaky Rayleigh wave and the direct acoustic wave, and their reflections. The leaky Rayleigh wave propagates along concrete surface and then leaks into air at the leaky angle, and the arrival time to the microphone is a linear function of the offset distance. Because the distance between the accelerometer and the microphone was kept constant during the test, the leaky Rayleigh wave arrival time difference between these two sensors is a constant and is dictated by the microphone height and leaky angle. On the other hand, the direct acoustic wave generated by the impact travels through the air, and the arrival time to the microphone is a quadratic function of the horizontal offset distance. Figure 4(b) shows the amplitude spectra for different offsets. It is observed

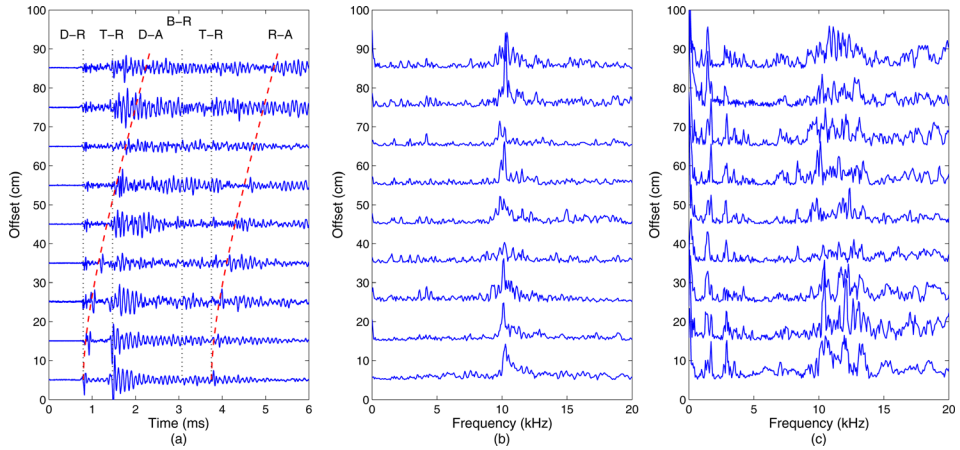

Fig. 4. (Color online) (a) Time signals and (b) spectra from different offset distance. Expected arrival times for leaky Rayleigh wave, acoustic wave and their reflection are shown as dashed lines. *D-R*, *T-R*, and *B-R* represent the direct leaky Rayleigh wave and its reflection from the reflector and the plate surface, respectively. *D-A* and *R-A* represent the direct and reflected (from the reflector) acoustic waves. (c) Spectra of signals taken by a microphone without the reflector from different offsets (height 0.5 cm).

that as the offset increases, the microphone consistently captures the sharp peak at the S_1ZGV mode frequency. This is caused by the large energy collecting area of the reflector and the multiple reflections between the reflector and the slab surface. For comparison purpose, Fig. 4(c) shows the spectra measured by the microphone without reflector from the same offset distances. At large offsets, the spectra show much weaker peaks at the S_1ZGV frequency and higher noise level on other frequency contents. The comparison verifies that the reflector selectively amplifies the S_1ZGV mode.

5. Conclusions

In this letter, the use of a parabolic reflector on the ACIE test is reported. Comparison of test results gathered with and without the reflector shows the significant gain on the S_1ZGV frequency content in the signal when using a reflector. The parabolic reflector not only focuses the S_1ZGV wave into the focal area, but also reflects the waves back to the test surface and creates multiple reflections which maintains acoustic energy near the microphone for longer periods of time. Both of these phenomena lead to enhanced signal energy at the S_1ZGV frequency which was experimentally verified. Further, the parabolic reflector helps increase signal energy of the S_1ZGV mode when the sensor is far from the test surface or from the impact source by collecting signal from a large area surrounding the sensor. With the offset test setup, the first arrival in the time domain signal was identified as the leaky surface wave. This work therefore suggests that a parabolic reflector would be effective for air-coupled sensing in both IE and surface wave tests.

Acknowledgments

This study was supported by NIST Technology Innovation Program (TIP).

References and links

Clorennec, D., Prada, C., and Royer, D. (**2007**). "Local and noncontact measurements of bulk acoustic wave velocities in thin isotropic plates and shells using zero group velocity Lamb modes," J. Appl. Phys. **101**(3), 034908.

Gibson, A., and Popovics, J. S. (**2005**). "Lamb wave basis for impact-echo method analysis," J. Eng. Mech. **131**(4), 438–443.

Holland, S. D., and Chimenti, D. E. (**2004**). "High contrast air-coupled acoustic imaging with zero group velocity lamb modes," Ultrasonics **42**(1-9), 957–60.

Holland, S. D., and Chimenti, D. E. (**2003**). "Air-coupled acoustic imaging with zero-group-velocity Lamb modes," Appl. Phys. Lett. **83**(13), 2704–2706.

Prada, C., Clorennec, D., and Royer, D. (**2008**). "Local vibration of an elastic plate and zero-group velocity Lamb modes," J. Acoust. Soc. Am. **124**(1), 203–12.

Sansalone, M. J., and Carino, N. J. (**1986**). "Impact-echo: A method for flaw detection in concrete using transient stress waves," U.S. Dept. of Commerce, National Bureau of Standards, Center for Building Technology, Structures Division, Gaithersburg, MD, NBSIR 86-3452.

Zhu, J., and Popovics, J. S. (**2005**). "Non-contact imaging for surface-opening cracks in concrete with air-coupled sensors," Mater. Struct. **38**(283), 801–806.

Zhu, J., and Popovics, J. S. (**2007**). "Imaging concrete structures using air-coupled impact-echo," J. Eng. Mech. **133**(6), 628–640.

Zhu, J., and Popovics, J. S. (**2002**). "Non-contact detection of surface waves in concrete using an air-coupled sensor," Rev. Quant. Nondestr. Eval. **21**, 1261–1268.